Preprints of the 18th IFAC World Congress
Milano (Italy) August 28 - September 2, 2011

Adaptive Force Control of Automotive Clutch Actuator System with Self-Energizing Effect

Jinsung Kim * **Seibum B. Choi** *,⋆

* *Department of Mechanical Engineering, KAIST (Korea Advanced Institute of Science and Technology), Daejeon, Korea (e-mail: {jsk, sbchoi}@kaist.ac.kr).*

Abstract: Advanced automatic transmissions in recently developed vehicles are generally equipped with the servo-actuated clutch system. In that system, the normal force or the clutch torque control of electric motor type actuators is quite difficult because the measurement of the clutch torque is impractical in the real environment. Particularly, the system studied in this paper is equipped with an actuator utilizing self-energizing effect to reinforce the clutch force with much less actuation energy. Since such a system includes torque amplification mechanism, some parametric uncertainties in the clutch torque controller are also amplified. Adaptive sliding mode control scheme for a robust clutch control is proposed to ensure the smooth engagement without torque measurement. The friction coefficient of the clutch surface is estimated to control the engagement torque properly.

Keywords: Adaptive control, Automotive control, Force control, Servomotor actuators, Parameter estimation

1. INTRODUCTION

The clutch plays an important role in power transmission from the engine to the wheel of automotive systems. To meet some requirements such as driving comfort, the clutch operation should be performed accurately. In manual transmission (MT) vehicles, the clutch engagement can be determined by driver's own intention and skill alone so that the shift feeling is not an issue. Automatic Transmission (AT) does not require significant consideration of clutch comfort because torque converters bring about smoothed operation although there is some energy loss. On the other hand, recent progress in advanced transmission technology such as Automated Manual Transmissions (AMT) or Dual Clutch Transmissions (DCT) makes clutch control strategy important especially when a dry friction clutch is adopted. In such systems, the clutch and the gear shifting mechanism are servo-controlled by electrical or hydraulic actuators.

Since undesirable clutch slip and over-actuation may lead to the degradation of engagement quality, the clutch torque has to be controlled to ensure the engagement operation without slip and satisfy driver's comfort (Kim and Choi (2010)). Moreover, it is especially problematic to control the engagement of dry clutch systems due to the discontinuous characteristic compared with wet clutches.

Various kinds of methods have been proposed for dry clutch engagement. In Serrarens et al. (1999), the dynamic behavior of automotive dry clutches and a decoupling proportional-integrative controller for engine and torque control. In Heijden et al. (2007), Garofalo et al. (2002), Dolcini et al. (2005), and Glielmo and Vasca (2000), optimal control approaches are proposed by the development of a linear quadratic regulator and a model predictive control. Nonlinear control method based on backstepping technique (Fredriksson and Egardt (2000)) and a hierarchical approach consists of decoupled feedback loops have been proposed for gearshift control (Glielmo et al. (2006)), respectively. Several researches introduced above are based on the assumption that the clutch actuator works well without any limitation. But, actuator dynamic behavior and physical limitations are very important since it is critical to determine transient response during the clutch engagement. In order to consider the actuator dynamics, the hydraulic component models for clutch positioning system are derived as well as driveline models in Horn et al. (2003), Lucente et al. (2007), and Montanari et al. (2004). On the other hand, This paper provides the development of the normal force and the clutch torque controller considering actuator dynamics. The clutch actuator system taken into account in this research is based upon the self-energizing mechanism suggested by Kim and Choi (2011). Compared with conventional clutch actuators, it has the advantage of reducing actuation energy significantly by reinforcing the engagement force. However, since there are uncertainties in the actuator dynamic model and the clutch torque parameters, the controllers designed for general purpose can suffer the degradation of performance.

In the self-energizing clutch actuator system, where the clutch torque is amplified by self-energizing mechanism, parametric uncertainties are also amplified. Thus, the control performance can be deteriorated. To solve this problem, a sliding mode controller is designed which is robust to modeling uncertainties. Also an adaptation scheme to estimate the friction coefficient of the clutch surfaces is developed.

2. DYNAMIC MODEL

2.1 Full System Model

In this section, the dynamic models for the clutch actuator with self-energizing effect are presented to describe essential dynamics of physical systems. The overall system can be divided into two parts: an electric motor and a mechanical clutch

⋆ Corresponding author

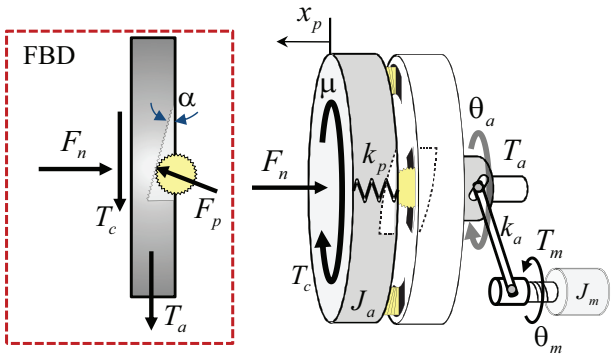

Fig. 1. Schematic of the equivalent clutch actuator model

subsystem. It will be used to design a controller to track the normal force and therefore the torque applied on the friction surface for the engagement or disengagement of the clutch.

The motor electric and mechanical equations are as follows, respectively.

$$L_m \frac{di_m}{dt} + R_m i_m + k_m \omega_m = u \tag{1}$$

$$J_m \frac{d\omega_m}{dt} + T_{fm}(\omega_m, z_m) + T_L = T_m \tag{2}$$

In (1), u is the voltage applied to the motor, i_m the motor current, R_m the resistance, L_m the inductance, and k_m the back electromotive force constant. In equation (2). J_m is the motor moment of inertia, ω_m the rotor speed, T_L the load torque, and $T_m = k_t i_m$ the motor torque. The nonlinear motor friction torque T_{fm} is modeled by the LuGre friction model in Wit et al. (1995) as

$$\begin{aligned} T_{fm}(\omega_m, z_m) &= \sigma_{0m} z_m + \sigma_{1m} \dot{z}_m + \sigma_{2m} \omega_m \\ \frac{dz_m}{dt} &= \omega_m - \frac{|\omega_m|}{g_m(\omega_m)} z_m \\ \sigma_0 g_m(\omega_m) &= f_{cm} + (f_{sm} - f_{cm}) e^{-(\omega_m/\omega_{ms})^2} \end{aligned} \tag{3}$$

where, z denotes the internal friction state, g_m the nonlinear function for the stribeck effect of dry friction, f_{cm} the Coulomb friction level, f_{sm} the static friction level, and ω_{ms} the stribeck velocity. In (3), σ_{0m}, σ_{1m}, and σ_{2m} are unknown friction parameters that represent bristle stiffness, bristle damping, and viscous coefficient, respectively.

The fixed plate shown in Fig. **??** is interposed between the clutch cover and the friction disks in order to adjust the axial displacement of the actuation plate while rotating at the same time. In free space, the rotational equation of motion for the actuation plate without the clutch engagement torque is described as

$$J_a \dot{\omega}_a = T_a - T_{fa}(\omega_a, z_a) \tag{4}$$

where, J_a is the moment of inertia of the actuation plate. Since the pinions are constrained by two supporting plates and the pinion guide, the motion of them coincides with the actuation plate. Thus, it is reasonable to assume that the inertia of the pinions is lumped into that of the actuation plate. In (4), the frictional torque T_{fa} on the worm shaft is represented by

$$\begin{aligned} T_{fa}(\omega_a, z_a) &= \sigma_{0a} z_a + \sigma_{1a} \dot{z}_a + \sigma_{2a} \omega_a \\ \frac{dz_a}{dt} &= \omega_a - \frac{|\omega_m|}{g_a(\omega_a)} z_a \\ \sigma_0 g_a(\omega_a) &= f_{ca} + (f_{sa} - f_{ca}) e^{-(\omega_a/\omega_{as})^2} \end{aligned} \tag{5}$$

where, all parameter notations are the same as (3) with the use of the subscript 'a' instead of 'm'.

The equivalent torsional stiffness k_a of the mechanical link between the lever and the worm shaft can be represented as a series of the torsional stiffness of the ball-screw k_{bs} and the lever k_l as shown in Ebrahimi and Whalley (2000).

$$k_a = \left(\frac{1}{k_{bs}} + \frac{1}{k_l} \right)^{-1} \tag{6}$$

Then, the driving torque T_a is transferred from the motor to the mechanical actuator due to an elastic deformation with the equivalent torsional stiffness k_a as

$$T_a = k_a \left(\frac{\theta_m}{N_g} - \theta_a \right) \tag{7}$$

where, θ_a is the actuator angular position, and N_g the equivalent conversion ratio between the motor and the actuator angular position. Since the load torque T_L in the motor dynamics (2) is the driving torque T_a in (4) and (7), the following relationship is satisfied, i.e., $T_L = T_a / N_g$.

When the clutch is in contact with the surface for engagement operation, the clutch torque and the reinforcement torque is added in (4) as shown in Fig. **??**. Therefore, the equation of motion for the actuation plate in the slip phase is represented by

$$J_a \dot{\omega}_a = T_a + T_c - 2 r_p F_p \sin\alpha - T_{fa}(\omega_a, z_a) \tag{8}$$

where, T_c is the clutch torque, F_p the reaction force on the rack and pinion surface, r_p and α are the radius of bevel gear position and the inclined surface angle, which is fixed and engraved on the actuation plate and the fixed plate, respectively. For the positive slip phase, the clutch torque T_c is obtained as

$$T_c = \mu R_c F_n \tag{9}$$

where, μ is the dry friction coefficient, R_c the effective clutch radius, and F_n the applied normal force. Since there is rack and pinion mechanism, the relationship between F_p and F_n is determined by the inclined surface angle α as shown in Fig. **??**. As a result, F_p is:

$$F_p = \frac{F_n}{\cos\alpha}. \tag{10}$$

Note that the third term at the right hand side in (8) is related to self-energizing effect. The existence of rack and pinion mechanism can induce the reaction force F_p on the surface of the actuation plate and the fixed plate with respect to the applied normal force F_n.

The axial displacement of the actuation plate can be calculated through the geometric relation as shown in Fig. **??**. It is therefore given by

$$x_p = 2 r_p \theta_a \tan\alpha \tag{11}$$

where, θ_a is the angular position of the actuation plate. The normal force applied on the friction disk is

$$F_n = k_p x_p = 2 k_p r_p \theta_a \tan\alpha \tag{12}$$

where, k_p is the stiffness of the actuation plate. It is assumed that the normal force F_n is proportional to the actuator stroke x_p in axial direction.

According to (9), (10), and (12), then the actuator dynamics (8) in the positive slip phase can be rewritten as

$$J_a\dot{\omega}_a = \mu R_c F_n + T_a - 2r_p \tan\alpha F_n - T_{fa}(\omega_a, z_a). \tag{13}$$

The feasibility of the system model described in this section is partially discussed in Kim and Choi (2011).

2.2 Simplified Model for Control

The dynamic model of the clutch actuator introduced in the previous subsection is not useful for the purpose of control due to its complexity. In the subsequent control development, sliding mode control scheme will be employed. Since higher system order may cause increased dimensionality of the sliding hyperplane, it results in the degradation of control performance in practical point of view if the relative order of the system model for control is more than second order.

It is necessary to make some hypothesis to simplify the actuator model. Some reasonable assumptions are:

a) the electrical dynamics of the DC motor is faster than the mechanical motions.
b) the bandwidth of the actuation plate is very high, and the rotating angle of it is very small

The first assumption means that the inductance of the DC motor could be neglected due to the relation $L_m \ll J_m$ (Utkin et al. (1999)). Thus, the dynamic equation (1) is converted into an algebraic equation as follows.

$$u = R_m i_m + k_m \omega_m \tag{14}$$

Also, the rotating motion of the actuation plate is relatively small compared with that of the motor. The assumption is valid if the stiffness of the actuation plate is very large. Therefore, the dynamics of the actuation plate is negligible. Consequently, equation (13) can be rewritten as

$$2r_p F_n \tan\alpha = T_a + \mu R_c F_n \tag{15}$$

Combining (7) and (15) gives a single equation for the normal force:

$$F_n = \frac{k_a(\theta_m/N_g - \theta_a)}{2r_p \tan\alpha - \mu R_c} \tag{16}$$

The expressions for the normal force shown in (12) and (16) are combined into the relationship between the angular position of the motor and that of the actuation plate.

$$\theta_a = \frac{k_a}{N_g(k_b + k_a)}\theta_m \tag{17}$$

where the auxiliary function k_b is defined for notational simplicity as

$$k_b \triangleq \xi(\mu)(2r_p k_p \tan\alpha) = \xi(\mu) k_p \beta, \tag{18}$$

$$\xi(\mu) \triangleq (2r_p \tan\alpha - \mu R_c) = (\beta - \mu R_c), \tag{19}$$

$$\beta \triangleq 2r_p \tan\alpha. \tag{20}$$

Substituting equation (17) in (16) derives an equation for the relationship between the normal force and the motor position.

$$F_n = \frac{k_a}{\xi(\mu)}\left[\frac{k_b}{N_g(k_b + k_a)}\right]\theta_m \tag{21}$$

The above equation is applied to convert desired normal force to desired motor position which will be used in the following section. The steady-state friction model can be obtained by

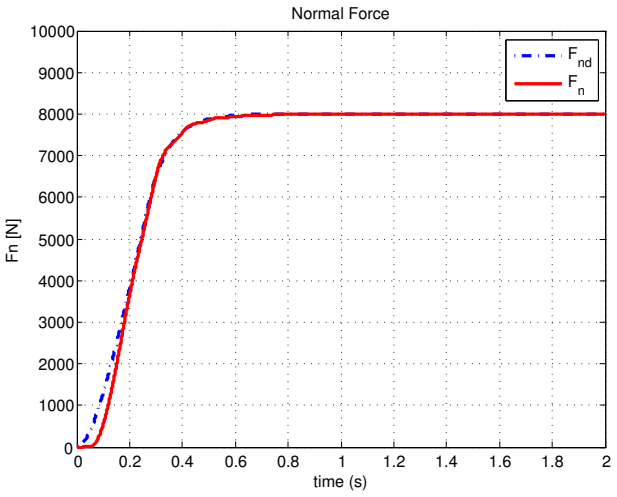

Fig. 2. Normal force control : sliding mode control with smoothed trajectory (Dash-dotted: smoothed reference , Solid: simulation)

setting $\dot{z} = 0$. Accordingly, the following linear-in-parameters model depending only on the velocity is given by

$$T_f'(\omega_m) = \phi_1 \mathrm{sgn}(\omega_m) + \phi_2 \omega_m \tag{22}$$

$$\phi_1 \triangleq \sigma_0 g(\omega_m), \quad \phi_2 \triangleq \sigma_2$$

where the detailed simplification process can be found in Wit et al. (1995). Although, the worm shaft friction is neglected in (15), it may affect the motor rotation so that the newly defined variables ϕ_1 and ϕ_2 include this frictional effect. Thus, a simplified model can be derived with respect to the motor states. Combining equation (2), (14), (15), (17), and (22) yields

$$\dot{\omega}_m + q\omega_m + T_f'(\omega_m) + r\theta_m + d = pu \tag{23}$$

where, the auxiliary functions are

$$p \triangleq \frac{k_t}{J_m R_m}, \tag{24}$$

$$q \triangleq \frac{1}{J_m}\left(\frac{k_t k_m}{R_m}\right), \tag{25}$$

$$r \triangleq \frac{k_a k_b}{J_m {N_g}^2 (k_b + k_a)} = w\left(\frac{k_b}{k_b + k_a}\right), \tag{26}$$

$$w \triangleq k_a/(J_m {N_g}^2), \tag{27}$$

$T_f'(\omega_m) = T_f(\omega_m)/J_m$ denotes the nonlinear friction model with uncertain parameters, and d the modeling uncertainty, respectively. Actual values of friction parameters are unknown but bounded to a range of known values to be estimated.

As a result, the order of the actuator system can be reduced to the second order as shown in (23). Consequently, the above equation is appropriately simplified for the purpose of controller design. It should be noted that this simplified model will only be used to design a controller. Thus, the plant model in the previous subsection remains in order to represent the entire system dynamics.

3. NORMAL FORCE CONTROL DEVELOPMENT

3.1 Sliding Mode Control

In order to ensure the clutch engagement, a sliding control law is proposed in this section. It is required to choose a sliding

surface to derive the control command. Although the goal of the control is to track the desired normal force for the appropriate clutch engagement operation, the normal force cannot be directly chosen as an error variable because measuring it is quite difficult or too costly. Moreover, it is even more expensive to measure the clutch torque in commercial vehicle using torque transducers. On the other hand, a feedback signal for the controller obtained from motor position can be measured easily by using an encoder. Therefore, the motor position error is chosen to define a sliding surface instead of the normal force or the clutch torque. Algebraic manipulation for converting normal force into motor position has been introduced in (21). It is assumed that the motor position is measurable, and its speed is obtained from numerical differentiation of the position signal. Define the desired motor position profile θ_{md}, the motor position error $\tilde{\theta}_m = \theta_m - \theta_{md}$, and its derivative $\dot{\tilde{\theta}}_m = \dot{\theta}_m - \dot{\theta}_{md}$, then a sliding surface is defined as

$$S \triangleq \dot{\tilde{\theta}}_m + \lambda \tilde{\theta}_m \tag{28}$$

where, λ is a constant design parameter. To make the surface attractive, the desired dynamics of the motor position error is defined as

$$\dot{S} = -KS \tag{29}$$

where K is a design parameter that determines the convergence speed of the surface to zero. The time derivative of the surface is

$$\dot{S} = \ddot{\tilde{\omega}}_m + \lambda \tilde{\omega}_m = \dot{\omega}_m - \dot{\omega}_{mr} \tag{30}$$

where $\tilde{\omega}_m = \dot{\theta}_m - \dot{\theta}_{md}$, and $\dot{\omega}_{mr} = \dot{\omega}_{md} - \lambda \tilde{\omega}_m$. Substituting the actual dynamics (23) into (30) yields the open-loop error system as

$$\dot{S} = pu - q\dot{\theta}_m - T_f'(\dot{\theta}_m) - r\theta_m - d - \dot{\omega}_{mr} \tag{31}$$

The motor voltage u can be chosen as the control input for the entire actuator system. Thus, the control input u can be derived as

$$u = \frac{1}{p}\left(\bar{q}\dot{\theta}_m + \bar{T}_f' + r\theta_m + \bar{d} + \dot{\omega}_{mr} - KS - M\mathrm{sgn}(S)\right) \tag{32}$$

where, $\bar{q}$, $\bar{T}_f'$, and $\bar{d}$ denote the nominal values of the parameters q, T_f', and d, respectively. And, M is a switching gain that will be determined later. In order to confirm the performance of the controller (32), the simulation is performed as shown in Fig. 1. Considering the limitation of the actuator bandwidth, a smoothed trajectory is chosen as a desired profile of the normal force. Fig. 1 shows a desirable performance with no overshoot and no steady-state error. The settling time is also short enough for the clutch control.

3.2 Friction Coefficient Adaptation

Although the controller designed for tracking the normal force applied on the clutch disk looks good enough to achieve the basic objective of a clutch system, parametric uncertainty should be taken into account in order to guarantee the robustness of the developed control system.

Due to the self-energizing nature of the developed system, small parametric uncertainty can cause the significant degradation of control performance such as a large steady state error or transient overshoot. Since the friction coefficient μ varies with the operating temperature and the material properties, slip behavior of both sides of the clutch during engagement/disengagement operations cannot always be ideal.

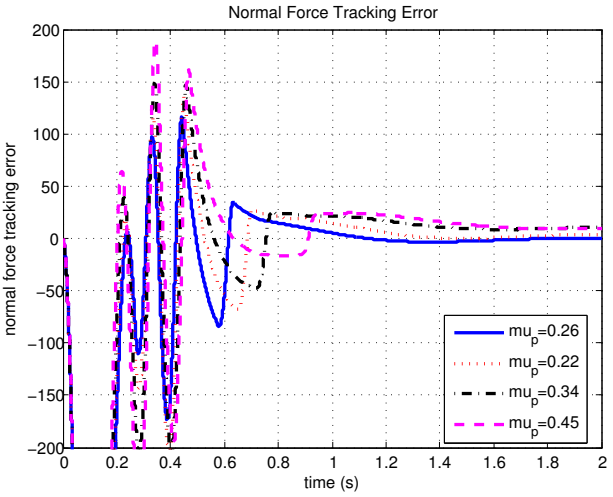

Fig. 3. Force tracking error [N] of sliding mode control in the presence of parametric uncertainty μ ($\mu_p \neq \mu_c$)

To illustrate this behavior, the following example is given as follows. Let μ_p denote the friction coefficient of the real plant and μ_c one used in control model. If μ_c is set to a nominal value 0.26 and μ_p is different values (i.e. 0.22, 0.34, and 0.45), this results in steady-state error of tracking the normal force in spite of large feedback gain K as shown in Fig. 2. The reason for this error is that the value of friction coefficient used in the controller is fixed at a nominal value. Furthermore, because the normal force of the clutch is proportional to the stiffness of the actuation plate according to section 2, small error between them can cause a large error in the normal force as indicated in Fig. 2.

To solve this problem, adaptive control of friction coefficient μ will be designed. This strategy is motivated by the fact that the variation of the friction coefficient is related to the tracking error of the clutch slip speed. The control law (32) suggested in the preceding section is redefined with parametric uncertainty as

$$u = \frac{1}{p}\left(u_0 + u_a - KS - M\mathrm{sgn}(S)\right) \tag{33}$$

where

$$\begin{aligned} u_0 &= \bar{q}\dot{\theta}_m + \bar{d} + \dot{\omega}_{mr}, \\ u_a &= \hat{\phi}_1 \mathrm{sgn}(\dot{\theta}_m) + \hat{\phi}_2\dot{\theta}_m + \hat{r}\theta_m, \\ \hat{r} &= w\left(\frac{\hat{k}_b}{\hat{k}_b + k_a}\right), \qquad (34) \\ \hat{k}_b &\triangleq \xi(\hat{\mu})k_p\beta. \qquad (35) \end{aligned}$$

Here, $\hat{r}$ includes an erroneous parameter $\hat{k}_b$ which is a function of $\hat{\mu}$ and other system parameters. The closed-loop system is rewritten by substituting equation (33) into (31) as

$$\dot{S} = -\tilde{q}\dot{\theta}_m - \tilde{\phi}_1\mathrm{sgn}(\dot{\theta}_m) - \tilde{\phi}_2\dot{\theta}_m - \tilde{r}\theta_m - \tilde{d} - KS - M\mathrm{sgn}(S) \tag{36}$$

where, $\tilde{q} = q - \bar{q}$, $\tilde{\phi}_i = \phi_i - \hat{\phi}_i$ $(i = 1,2)$, $\tilde{r} = r - \hat{r}$ and $\tilde{d} = d - \bar{d}$ are the errors between the real and the nominal parameters. As

shown in (34), since $\hat{r}$ is a function of various parameters including parameter uncertainty μ, this problem can be classified as a nonlinearly parameterized system.

Based upon above definition of r, a modified adaptation law is derived as

$$\dot{\hat{r}} = -\varepsilon\theta_m S \tag{37}$$

where ε is a positive constant adaptive gain. Note that $\hat{r}$ can be assumed as a slowly varying parameter so that the time derivative it to be $\dot{\tilde{r}}_n = -\dot{\hat{r}}_n$. In addition, adaptation laws for compensating nonlinear friction in the system are given with initial conditions as

$$\dot{\hat{\phi}}_1 = -\delta_1 \mathrm{sgn}(\dot{\theta}_m)S, \quad \hat{\phi}_1(0) = f_s/J_m, \tag{38}$$

$$\dot{\hat{\phi}}_2 = -\delta_2 \dot{\theta}_m S, \quad \hat{\phi}_2(0) = b_m/J_m \tag{39}$$

where, δ_1 and δ_2 are design parameters for determining adaptation rate.

3.3 Stability Analysis

Theorem 1. Under the desired trajectory θ_{md} is sufficiently bounded and smooth (i.e. $\theta_{md}, \dot{\theta}_{md}, \ddot{\theta}_{md} \in \mathcal{L}_\infty$), the controller given by (33), (37), (38) and (39) ensures the asymptotic tracking of the normal force control system in the sense that

$$\tilde{\theta} \to 0, \quad \tilde{\mu} \to 0 \quad as \quad t \to \infty$$

provided the positive adaptive gains ε, δ_1, and δ_2 are properly chosen, and the switching gain M is selected according to the following condition

$$|M| \geq |\tilde{q}\dot{\theta}_m + \tilde{d}|.$$

Proof. Let $V \in \mathbb{R}$ denote a positive definite Lyapunov function candidate

$$V = \frac{1}{2}S^2 + \frac{1}{2\varepsilon}\tilde{r}^2 + \frac{1}{2\delta_1}\tilde{\phi}_1^2 + \frac{1}{2\delta_2}\tilde{\phi}_2^2, \tag{40}$$

and the time derivative of (40) is given by

$$\dot{V} = S\dot{S} + \frac{1}{\varepsilon}\tilde{r}\dot{\tilde{r}} + \frac{1}{\delta_1}\dot{\tilde{\phi}}_1^2 + \frac{1}{\delta_2}\dot{\tilde{\phi}}_2^2. \tag{41}$$

Using (33), and (36), it is rewritten as

$$\begin{aligned}\dot{V} &= S[-\tilde{q}\dot{\theta}_m - \tilde{\phi}_1 sgn(\dot{\theta}_m) - \tilde{\phi}_2\dot{\theta}_m - \tilde{r}\theta_m - \tilde{d} - KS - M\mathrm{sgn}(S)] \\ &\quad -\frac{1}{\varepsilon}\tilde{r}\dot{\hat{r}} - \frac{1}{\delta_1}\tilde{\phi}_1\dot{\hat{\phi}}_1 - \frac{1}{\delta_2}\tilde{\phi}_2\dot{\hat{\phi}}_2 \\ &= -KS^2 - S\left[\tilde{q}\dot{\theta}_m + \tilde{d}\right] + M|S| - \tilde{r}\left[\theta_m S + \frac{\dot{\hat{r}}}{\varepsilon}\right] \\ &\quad -\tilde{\phi}_1\left[S\mathrm{sgn}(\dot{\theta}_m) + \frac{\dot{\hat{\phi}}_1}{\delta_1}\right] - \tilde{\phi}_2\left[\theta_m S + \frac{\dot{\hat{\phi}}_2}{\delta_2}\right]\end{aligned} \tag{42}$$

where the design parameter M is selected to satisfy the inequality $|M| \geq |\tilde{q}\dot{\theta}_m + \tilde{d}|$. By utilizing (37), (38), and (39), the following inequality is obtained as

$$\dot{V} \leq -KS^2. \tag{43}$$

Therefore, the time derivative of $\dot{V}$ is negative semi-definite.

Since the purpose of this scheme is the good estimation of the friction coefficient $\hat{\mu}$, it is required to derive an equation to estimate μ. The time derivative of $\hat{r}$ can be obtained from (34) as,

$$\dot{\hat{r}} = w\frac{d}{dt}\left(\frac{\hat{k}_b}{\hat{k}_b + k_a}\right) = w\frac{k_a}{(\hat{k}_b + k_a)^2}\dot{\hat{k}}_b. \tag{44}$$

The equation for $\dot{\hat{k}}_b$ is rewritten by

$$\dot{\hat{k}}_b = \frac{(\hat{k}_b + k_a)^2}{wk_a}\dot{\hat{r}} \tag{45}$$

k_b is defined as a function of μ in (18) for the notational simplicity. The estimated versions of k_b and its time derivative are:

$$\hat{k}_b = \hat{\xi}(\alpha, \hat{\mu})(k_p\beta) \tag{46}$$

$$\dot{\hat{k}}_b = -(k_p R_c \beta)\dot{\hat{\mu}}. \tag{47}$$

Combining (45) and (47) yields

$$\dot{\hat{\mu}} = -\frac{(\hat{k}_b + k_a)^2}{wk_a k_p R_c \beta}\dot{\hat{r}}. \tag{48}$$

Finally, the adaptation law in terms of $\hat{\mu}$ is given by

$$\dot{\hat{\mu}} = -\frac{\{\hat{\xi}(\hat{\mu})(k_p\beta) + k_a\}^2}{wk_a k_p R_c \beta}\dot{\hat{r}}. \tag{49}$$

Generally, the control system property of interest is asymptotic stability. In (42), $\tilde{r}$, and S are bounded. A simple calculation shows that $\ddot{V}$ is also bounded. Therefore, Barbalat's Lemma can be applied (Slotine and Li (1991)). It subsequently implies

$$\lim_{t\to\infty} \tilde{r} = \lim_{t\to\infty} S = 0. \tag{50}$$

Therefore, $\hat{r} \to r$, and finally $\hat{k}_b \to k_b$. It means that the unknown parameter $\hat{\mu}$ converges to an actual parameter μ when the time goes to infinity. Another condition to check for the parameter convergence is the persistence of excitation. The adaptation law suggested is valid only if the persistence of excitation (PE) condition is satisfied. Since the motor angular position keeps $\theta_m > 0$ or $\theta_m < 0$, the PE condition is satisfied.

3.4 Simulation Results

The results of adaptive sliding mode control are shown in Fig. 3a, where the tracking performance is quite robust especially for the friction coefficient of the clutch disk. There are no steady-state errors as shown in Figure 3b. In these simulations, the plant parameters are set to 0.22, 0.26, 0.34, and 0.45 to testify robustness of the controller. The initial value of the adaptive law is fixed in its nominal value of 0.35 for comparison. The results in Fig. 4 show that $\hat{\mu}$ converges to the real parameter μ_p which is set to corresponding values in each case. Compared with Fig 2, the normal force errors converge to zero in spite of friction coefficient variations. These results show that adaptation algorithm suggested in (32), (37), (38), and (38) further improves the performance of the sliding control law.

4. CONCLUSIONS

In this paper, a control scheme for the clutch actuator system with self-energizing mechanism is developed based on sliding mode control. Since the variation of the friction coefficient may lead to undesirable large tracking error due to the self-energizing effect, it should be taken into account to ensure the robust control during fast engagement of the clutch. The proposed adaptation algorithm considers not only parametric

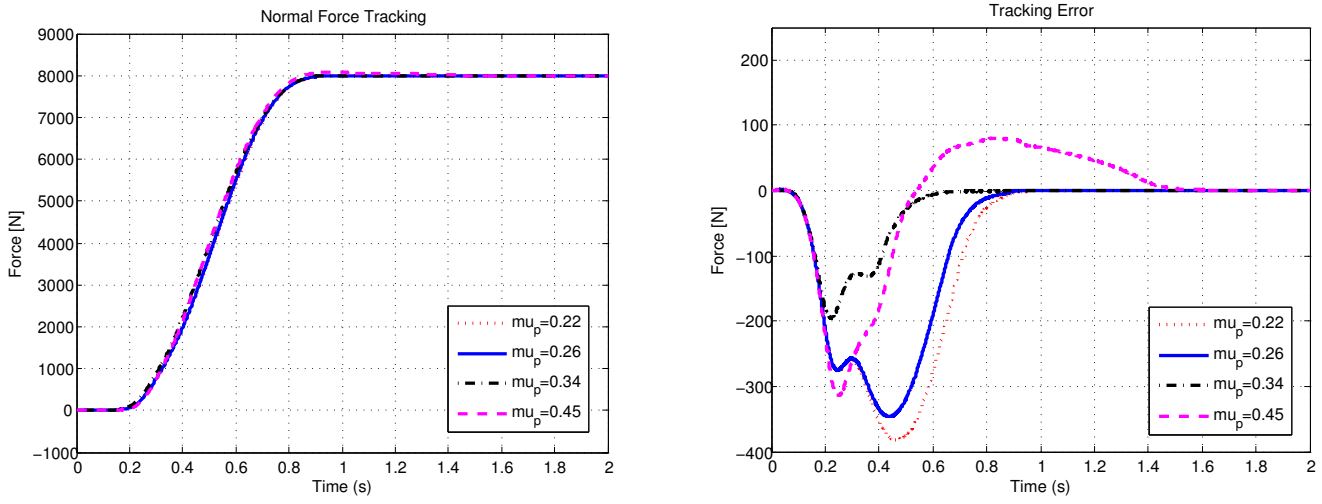

Fig. 4. Adaptive sliding mode control: (a) $\hat{\mu}$ Parameter adaptation ($\mu_p \neq \mu_c$). (b) $F_n - F_{nd}$ with $\hat{\mu}$ Parameter adaptation ($\mu_p \neq \mu_c$).

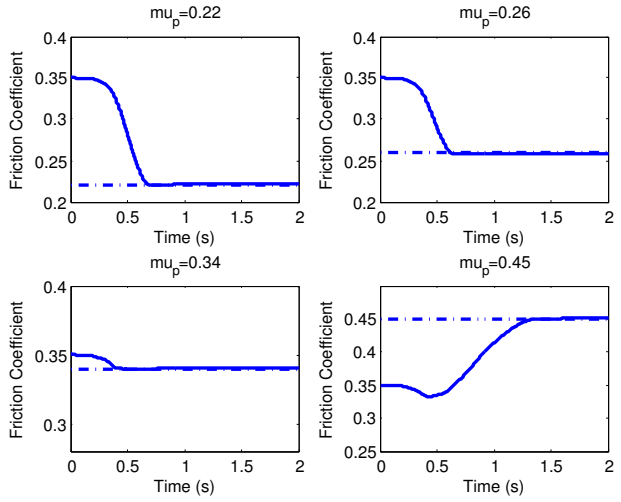

Fig. 5. Friction coefficient adaptation : $\mu_p = 0.22, 0.26, 0.34, 0.45$(dashed), and $\hat{\mu}_{c0} = 0.35$(nominal value, solid)

uncertainties but also clutch engagement operations. The simulation results show that performance of the sliding controller can be improved significantly when it is combined with the adaptation algorithm. In future works, experimental validation is needed to verify the control performance.

REFERENCES

Dolcini, P., Bechart, H., and de Wit, C.C. (2005). Observer-based optimal control of dry clutch engagement. In *Proc. of the 44th IEEE Conference on Decision and Control, and the European Control Conference*. Seville, Spain.

Ebrahimi, M. and Whalley, R. (2000). Analysis, modeling and simulation of stiffness in machine tool drives. *Computers & Industrial Engineering*, 38(1), 93–105. doi:10.1016/S0360-8352(00)00031-0.

Fredriksson, J. and Egardt, B.S. (2000). Nonlinear control applied to gearshifting in automated manual transmission. In *Proc. of the IJCEE, Conference on Decision and Control*. Sydney, Austrailia.

Garofalo, F., Glielmo, L., Iannelli, L., and Vasca, F. (2002). Optimal tracking for automotive dry clutch engagement. In *Proc. of IFAC 15th Triennial World Congress*. Barcelona, Spain.

Glielmo, L., Iannelli, L., Vacca, V., and Vasca, F. (2006). Gearshift control for automated manual transmission. *IEEE/ASME Trans. Mechatron.*, 11(1), 17–26.

Glielmo, L. and Vasca, F. (2000). Engagement control for automotive dry clutch. In *Proc. of 2000 American Control Conference*. Chicago, Illinois.

Heijden, A., Serrarens, A., Camlibel, M., and Nijmeijer, H. (2007). Hybrid optimal control of dry clutch engagement. *Int. J. Control*, 80(11), 1717–1728.

Horn, J., Bambergera, J., Michaub, P., and Pindlb, S. (2003). Flatness-based clutch control for automated manual transmissions. *Control Engineering Practice*, 11, 1353–1359.

Kim, J. and Choi, S.B. (2010). Control of dry clutch engagement for vehicle launches via a shaft torque observer. In *Proceedings of 2010 American Control Conference*, 676–681.

Kim, J. and Choi, S.B. (2011). Design and modeling of a clutch actuator system with self-energizing mechanism. *IEEE/ASME Trans. Mechatron.* Accepted for publication.

Lucente, G., Montanari, M., and Rossi, C. (2007). Modelling of an automated manual transmission system. *Mechatronics*, 17, 73–91.

Montanari, M., Ronchi, F., Rossi, C., Tilli, A., and Tonielli, A. (2004). Control and performance evaluation of a clutch servo system with hydraulic actuation. *Control Eng. Pract.*, 12, 1369–1379.

Serrarens, A., Dassen, M., and Steinbuch, M. (1999). Simulation and control of an automotive dry clutch. In *Proc. of the 2004 American Control Conference*, volume 5, 4078–4083. Boston, Massachusetts.

Slotine, J.J.E. and Li, W. (1991). *Applied Nonlinear Control*. Prentice-Hall, Englewood Cliffs, NJ.

Utkin, V., Guldner, J., and Shi, J. (1999). *Sliding Mode Control in Electromechanical Systems*. Taylor & Francis.

Wit, C.D., Olsson, H., Astrom, K., and Lischinsky, P. (1995). A new model for control of systems with friction. *IEEE Trans. Automat. Contr.*, 40(3), 419–425.